Journal of Photochemistry and Photobiology A: Chemistry 224 (2011) 91–101

Contents lists available at SciVerse ScienceDirect

Journal of Photochemistry and Photobiology A: Chemistry

journal homepage: www.elsevier.com/locate/jphotochem

A comparative study of ^{1}H NMR and sensitized visible light emission of an extended series of dinuclear lanthanide complexes☆,☆☆

Mir Irfanullah, K. Iftikhar*

Laboratory of Lanthanide Chemistry, Department of Chemistry, Jamia Millia Islamia, New Delhi 110 025, India

ARTICLE INFO

Article history:
Received 24 March 2011
Received in revised form 13 August 2011
Accepted 9 September 2011
Available online 16 September 2011

Keywords:
Dinuclear lanthanide complex
Bipyrimidine
Paramagnetic NMR
Luminescence
Energy transfer

ABSTRACT

An extended series of dinuclear lanthanide β-diketonate complexes of the type $[Ln_2(fod)_6(\mu\text{-bpm})]$ (Ln = Nd, Sm, Eu, Gd, Tb, Dy, Ho, Er, Tm, Yb and Lu; fod is the anion of 6,6,7,7,8,8,8-heptafluoro-2,2-dimethyl-3,5-octanedione; bpm = 2,2′-bipyrimidine) and polymeric complexes of the type $[Ln(fod)_3(bpm)]_n$ (Ln = La and Pr) have been isolated and thoroughly investigated in solution, by means of ^{1}H NMR and steady-state luminescence spectroscopies. The ^{1}H NMR chemical shift for the protons of paramagnetic complexes is analysed and discussed. The typical sensitized red, pink, green and yellow emission of Pr(III)/Eu(III), Sm(III), Tb(III) and Dy(III) complexes, respectively, is observed upon the excitation of the coordinated ligands. The comparison of the steady-state luminescence intensities of the complexes reveals that ligand-to-metal energy transfer is most efficient in Eu(III) complex followed by Sm(III) and Pr(III) complexes. The Tb(III) and Dy(III) complexes show relatively weak luminescence due to inefficient energy transfer.

1. Introduction

The design and synthesis of lanthanide complexes with organic ligands is a fascinating area of research owing to the unique luminescence and paramagnetic properties associated with Ln(III) ions [1–3]. The luminescent lanthanide complexes find a range of applications such as light-emitting devices [4], sensors [5,6], liquid crystalline materials [7] and imaging agents [8]. The luminescence of lanthanide complexes can be tuned from visible to near infrared region of the spectrum simply by choice of the individual lanthanide. Provided that a suitable organic ligand coordinates to the lanthanide ion, red emission can be observed from europium(III) complexes, green emission from terbium(III), pink emission from samarium(III), yellow emission from dysprosium(III) and near infrared emissions from neodymium(III), erbium(III) and ytterbium(III). Several of the paramagnetic lanthanide β-diketonate chelates, especially Pr(III), Eu(III) and Yb(III) are useful as NMR shift reagents [9]. When an organic molecule with a second order NMR spectrum is coordinated to one of these complexes, the large magnetic moment of the ion causes displacement and spreading out of the spectrum making it amenable to a first order spectrum.

β-Diketones have been widely used in lanthanide chemistry and they give thermodynamically stable and photoluminescent compounds [6,10]. They have a typical strong π–π^* absorption band in the UV region and their excited states possess suitable energy levels to effectively sensitize the lanthanide luminescence. Moreover, the lipophilic shell formed by β-diketones around the lanthanide ions enables the dissolution of the chelates in non polar-solvents. Since lanthanide tris β-diketonates are coordinatively unsaturated, they can rapidly react with an additional neutral ligand such as 1,10-phenanthroline (phen) and 2,2′-bipyridyl (bpy) or their derivatives to form coordinatively saturated complexes [11–16]. However, if the neutral ligand offers two equivalent sites for the coordination, unique dinuclear lanthanide complexes could be obtained [6,17–19].

2,2′-Bipyrimidine (bpm) is a planar heterocyclic ligand which offers two equivalent NN chelating sites for the metal coordination. Apart from acting as neutral ancillary ligand, it can also link the two Ln(β-diketonate)$_3$ fragments to form facile dinuclear lanthanide(III) complexes [20–23]. The bpm has also been used to connect Ln(β-diketonate)$_3$ units with transition metal complexes to form heterodinuclear d/f complexes [24,25]. In these complexes, bpm has been used to connect the two metal sites in order to keep the metal–metal separation short and to facilitate d → f energy transfer. We have recently described in one of our preliminary

☆ Abstracted in part from the PhD thesis (2010) of Mir Irfanullah, Jamia Millia Islamia, New Delhi.

☆☆ Part of the work was supported by the UGC Special Assistance Programme to the Department of Chemistry (No. F.540/17/DRS/2007/SAP-1), which is gratefully acknowledged.

* Corresponding author. Tel.: +91 11 26837297; fax: +91 11 26980229/26982489.
E-mail address: kiftikhar@jmi.ac.in (K. Iftikhar).

1010-6030/$ – see front matter © 2011 Elsevier B.V. All rights reserved.
doi:10.1016/j.jphotochem.2011.09.011

communications [20] the synthesis of four new homodinuclear lanthanide complexes of the type $[Ln_2(fod)_6(\mu\text{-bpm})]$ (Ln = Nd, Eu, Tb, and Lu) in which bpm was employed to connect two coordinatively unsaturated $Ln(fod)_3$ chelates, where fod is the anion of 6,6,7,7,8,8,8-heptafluoro-2,2-dimethyl-3,5-octanedione. Subsequently, we studied the 4f–4f absorption and luminescence properties of the dinuclear Pr, Sm, Eu, Tb, Ho and Er complexes and their mononuclear $[Ln(fod)_3(bpy)]$ and $[Ln(fod)_3(phen)]$ analogues in a series of coordinating and non-coordinating solvents and have reported on the effect of environment on the 4f–4f absorption and emission process [26–29]. The role of ancillary ligands (phen, bpy and bpm) in the sensitization process of lanthanide luminescence was also investigated and discussed.

In the present work, we extend the synthesis to the rest of the lanthanides (except Ce and Pm) and report the ^1H NMR studies of all the diamagnetic and paramagnetic complexes of the series along with their parent $Ln(fod)_3$ chelates. The comparative emission study of visible light emitting complexes, Pr(III), Sm(III), Eu(III), Tb(III), Dy(III) and Tm(III) is also being reported by taking into consideration the triplet state of the coordinated ligands (fod and bpm) and the resulting energy gap between the triplet states and the emitting level of the Ln(III) ion.

2. Experimental

2.1. Materials

The commercially available chemicals that were used without further purification are: Ln_2O_3 (Ln = La, Nd, Sm, Eu, Gd, Tb, Dy, Ho, Er, Tm, Yb and Lu 99.99%) from Aldrich, Pr_6O_{11} from Leico Chem., USA. These oxides were converted to their corresponding chlorides, $LnCl_3{\cdot}nH_2O$, n = 6–7 by the standard procedure. 6,6,6,7,7,8,8,8-Heptafluoro-2,2-dimethyl-3,5-octanedione was purchased from Lancaster and 2,2′-bipyrimidine (bpm) was purchased from Aldrich. The $Ln(fod)_3$ chelates of La and all trivalent lanthanides (except Ce and Pm) were synthesized according to a published procedure [30] with the modification that $LnCl_3{\cdot}nH_2O$ was used instead of $Ln(NO_3)_3{\cdot}nH_2O$. All the solvents used in this study were AR/spectroscopic grade.

2.2. Methods

Infrared spectra were recorded on a Perkin-Elmer spectrum RX I FT-IR spectrophotometer as KBr disc in the range 4000–400 cm^{-1}. Elemental analyses were performed by Sophisticated Analytical Instrumentation Facility (SAIF), Punjab University, Chandigarh, India. Melting Points were recorded by conventional capillary method and confirmed by the DSC 6220 Exstar 6000 instrument from SIINT, Japan. The thermograms were recorded on TG/DTA 6300 Exstar 6000 from SIINT, Japan. The NMR spectra of the complexes and their parent chelates were recorded on a BRUKER AVANCE II 400 NMR Spectrometer. The electrospray ionisation mass spectra of the complexes in positive ion mode were recorded on a Waters Micromass Q-Tof Micro mass spectrometer. The magnetic susceptibilities were measured at Banaras Hindu University, Varanasi, India, at room temperature (30.5 °C) using the Faraday method with a Cahn-Ventron RM-2 balance standardized with $HgCo(NCS)_4$; diamagnetic corrections were calculated from Pascal constants. Steady state room temperature emission and excitation spectra (5×10^{-3} M) were recorded on Horiba Jobin Yvon Fluorolog 3–22 Spectrofluorimeter using a 450 W Xenon lamp as the excitation source and equipped with a R928P Hamamatsu photomultiplier tube as detector. The samples were contained in a 10 mm Quartz Fluorometer Cell with stopper from Starna Cells, Inc.

2.3. Syntheses of the complexes

The synthesis of the dinuclear complexes $[Nd_2(fod)_6(\mu\text{-bpm})]$ (mp = 203 °C) $[Eu_2(fod)_6(\mu\text{-bpm})]$ (mp = 216 °C) $[Tb_2(fod)_6(\mu\text{-bpm})]$ (mp = 219 °C) and $[Lu_2(fod)_6(\mu\text{-bpm})]$ (mp = 230 °C), is reported in our preliminary communication [20]. The synthesis of $[Pr(fod)_3(bpm)]_n$ (mp = 161 °C) and $[Sm_2(fod)_6(\mu\text{-bpm})]$ (mp = 212 °C), is given in Refs. [27,29]. The rest of the lanthanide complexes have been synthesized by similar procedure [20,27,29]. The synthesis of $[Er_2(fod)_6(\mu\text{-bpm})]$ given below is representative.

2.3.1. $[Er_2(fod)_6(\mu\text{-bpm})]$

$Er(fod)_3$ (0.3 g, 0.285 mmol) was dissolved in 40 mL of ethanol. To this solution was slowly added an ethanol solution of 2,2′-bipyrimidine (22.5 mg, 0.142 mmol of bpm in 20 mL ethanol) with continuous stirring. The reaction mixture was stirred for 4 h on the hot plate at 40 °C. The resulting solution (approx. 40 mL) was left for slow evaporation of the solvent at room temperature. The bright pink coloured crystals appeared after 24 h. The crystals were filtered off, washed twice with 0.5 mL hexane and cold ethanol and dried *in vacuo* over P_4O_{10}. The final product was obtained by repeated crystallization from absolute ethanol. Yield (0.28 g, 86%). Anal. calc. for $Er_2C_{68}H_{66}F_{42}O_{12}N_4$: C, 36.07; H, 2.93; N, 2.47. Found: C, 36.14; H, 2.95; N, 2.74%. TOF MS-ES$^+$: m/z 1074.1 $[Er(fod)_2(bpm)_2]^+$ (100%); m/z 1234.2 (54%); m/z 1394.3 (21%). Melting point 227 °C. $\chi_m{\cdot}T$ (31.5 °C) = 20.08 $cm^3\ mol^{-1}$ K.

2.3.2. $[La(fod)_3(bpm)]_n$

Colour (white). Yield (0.070 g, 41%). Anal. calc. for $LaC_{38}H_{36}F_{21}O_6N_4$: C, 38.59; H, 3.06; N, 4.73. Found: C, 38.69; H, 2.99; N, 4.48%. TOF MS-ES$^+$: m/z 1047.2 $[La(fod)_2(bpm)_2]^+$ (1%). Melting point 215 °C.

2.3.3. $[Pr(fod)_3(bpm)]_n$

Colour (green). Yield (0.11 g, 41%). Anal. calc. for $PrC_{38}H_{36}F_{21}O_6N_4$: C, 38.52; H, 3.06; N, 4.73. Found: C, 38.73; H, 3.06; N, 4.73%. TOF MS-ES$^+$: m/z = 889.1 $[Pr(fod)_2(bpm)]^+$ (4%); m/z = 1049.2 $[Pr(fod)_2(bpm)_2]^+$ (19%). Melting point 161 °C.

2.3.4. $[Gd_2(fod)_6(\mu\text{-bpm})]$

Colour (white). Yield (0.070 g, 81%). Anal. calc. for $Gd_2C_{68}H_{66}F_{42}O_{12}N_4$: C, 36.40; H, 2.96; N, 2.50. Found: C, 36.50; H, 2.93; N, 2.56%. TOF MS-ES$^+$: m/z 906.2 $[Gd(fod)_2(bpm)]^+$ (4%); m/z 1066.2 $[Gd(fod)_2(bpm)_2]^+$ (13%); m/z 1224.2 (16%); m/z 1384.2 (10%). Melting point 217 °C. $\chi_m{\cdot}T$ (31.5 °C) = 15.34 $cm^3\ mol^{-1}$ K.

2.3.5. $[Dy_2(fod)_6(\mu\text{-bpm})]$

Colour (white). Yield (0.095 g, 82%). Anal. calc. for $Dy_2C_{68}H_{66}F_{42}O_{12}N_4$: C, 36.23; H, 2.95; N, 2.48. Found: C, 36.33; H, 2.91; N, 2.61%. TOF MS-ES$^+$: m/z 912.2 $[Dy(fod)_2(bpm)]^+$ (1%); m/z 1072.2 $[Dy(fod)_2(bpm)_2]^+$ (10%); m/z 1230.3 (10%); m/z 1390.3 (6%); m/z 1405.3 (1%). Melting point 224 °C. $\chi_m{\cdot}T$ (31.5 °C) = 27.48 $cm^3\ mol^{-1}$ K.

2.3.6. $[Ho_2(fod)_6(\mu\text{-bpm})]$

Colour (light yellow). Yield (0.28, 86%). Anal. calc. for $Ho_2C_{68}H_{66}F_{42}O_{12}N_4$: C, 36.15; H, 2.94; N, 2.48. Found: C, 36.24; H, 2.98; N, 2.59%. TOF MS-ES$^+$: m/z 913.2 $[Ho(fod)_2(bpm)]^+$ (1%); m/z 1073.2 $[Ho(fod)_2(bpm)_2]^+$ (23%); m/z 1231.3 (15%); m/z 1391.3 (13%); m/z 1407.3 (5%). Melting point 225 °C. $\chi_m{\cdot}T$ (31.5 °C) = 28.50 $cm^3\ mol^{-1}$ K.

2.3.7. $[Tm_2(fod)_6(\mu\text{-bpm})]$

Colour (white). Yield (0.075 g, 82%). Anal. calc. for $Tm_2C_{68}H_{66}F_{42}O_{12}N_4$: C, 36.02; H, 2.93; N, 2.47. Found: C, 36.20; H, 2.92; N, 2.59%. TOF MS-ES$^+$: m/z 917.2 $[Tm(fod)_2(bpm)]^+$

(6%); *m/z* 1077.1 $[Tm(fod)_2(bpm)_2]^+$ (100%); *m/z* 1093.1 (12%); *m/z* 1235.2 (46%); *m/z* 1395.2 (15%). Melting point 227 °C. $\chi_m \cdot T$ (31.5 °C) = 14.92 $cm^3\ mol^{-1}$ K.

2.3.8. $[Yb_2(fod)_6(\mu\text{-}bpm)]$

Colour (white). Yield (0. 090 g, 82%). Anal. calc. for $Yb_2C_{68}H_{66}F_{42}O_{12}N_4$: C, 35.89; H, 2.92; N, 2.46. Found: C, 36.03; H, 2.95; N, 2.68%. TOF MS-ES$^+$: *m/z* 1082.2 $[Yb(fod)_2(bpm)_2]^+$ (33%); *m/z* 1098.1 (6%); *m/z* 1240.3 (11%); *m/z* 1400.2 (7%). Melting point mp 229 °C. $\chi_m \cdot T$ (31.5 °C) = 5.56 $cm^3\ mol^{-1}$ K.

3. Results and discussion

3.1. Synthesis and characterization

The syntheses of the complexes are outlined in Scheme 1. The reaction of $Ln(fod)_3$ chelates and bpm in 2:1 molar ratio in ethanol yields air and moisture stable dinuclear complexes of general formula $[Ln_2(fod)_6(\mu\text{-bpm})]$ (Ln = Nd, Sm, Eu, Gd, Tb, Dy, Ho, Er, Tm, Yb and Lu) in high yield (80–85%). The micro analyses results are in excellent agreement with the theoretically calculated values. Furthermore, the experimental room temperature (30.5 °C) molar magnetic susceptibility ($\chi_m \cdot T$) values of paramagnetic Nd–Nd, Gd–Gd, Tb–Tb, Dy–Dy, Ho–Ho, Er–Er, Tm–Tm and Yb–Yb complexes are 3.52, 15.34, 25.68, 27.48, 28.50, 20.08, 14.92 and 5.56 $cm^3\ mol^{-1}$ K, respectively. These values are close to that expected for two non-interacting Ln(III) ions. This confirms the presence of two paramagnetic ions per molecule in these complexes. The solubility of these complexes is lower than their mononuclear $[Ln(fod)_3(bpy)]$ and $[Ln(fod)_3(phen)]$ analogues [12]. It is important to note that $La(fod)_3$ and $Pr(fod)_3$ chelates could not form dinuclear complexes under similar reaction conditions; instead mononuclear complexes of the type $[Ln(fod)_3(bpm)]$ (Ln = La and Pr) were formed as shown by their elemental analysis. The yield of the mononuclear complexes is lower (*ca.* around 40%) and these were isolated as light powders and unreacted chelates are left in the reaction mixture after isolation of the complexes. The solubility of the La and Pr complexes is comparatively lower than the dinuclear complexes of the series.

3.2. IR spectra

The IR spectra of complexes exhibit very strong bands around 1620 and 1520 cm^{-1} which have been assigned to C=O and C=C stretching modes, respectively, and are typical of lanthanide tris β-diketonates [11,13] (Table S1 in Supporting information). However, the most striking difference noted in the IR spectra of the new complexes from their respective chelates is the appearance of the bands around 1580 cm^{-1} (strong) and 1540 cm^{-1} (weak) as an asymmetric doublet. These bands are due to the ring stretching modes of bipyrimidine and indicate that both sides of bpm are coordinated to the metal ions [31,32]. Another strong ring stretching band in free bipyrimidine at 1403 cm^{-1} is shifted to higher frequency as medium intensity band at ca. 1414 cm^{-1}.

It is noteworthy that the IR spectra of the lanthanum and praseodymium complexes are similar to the other complexes of the series displaying asymmetric doublet for the ring stretching modes of bpm. However, elemental analysis corresponds to the formula unit $[Ln(fod)_3(bpm)]$. Therefore, these complexes are presumed to adopt a coordination polymeric structure of the form $[Ln(fod)_3(bpm)]_n$ as shown in Chart 1. This presumption is strongly supported by the recent report on $[Nd(tta)_3(bpm)]$ [22] (tta is the

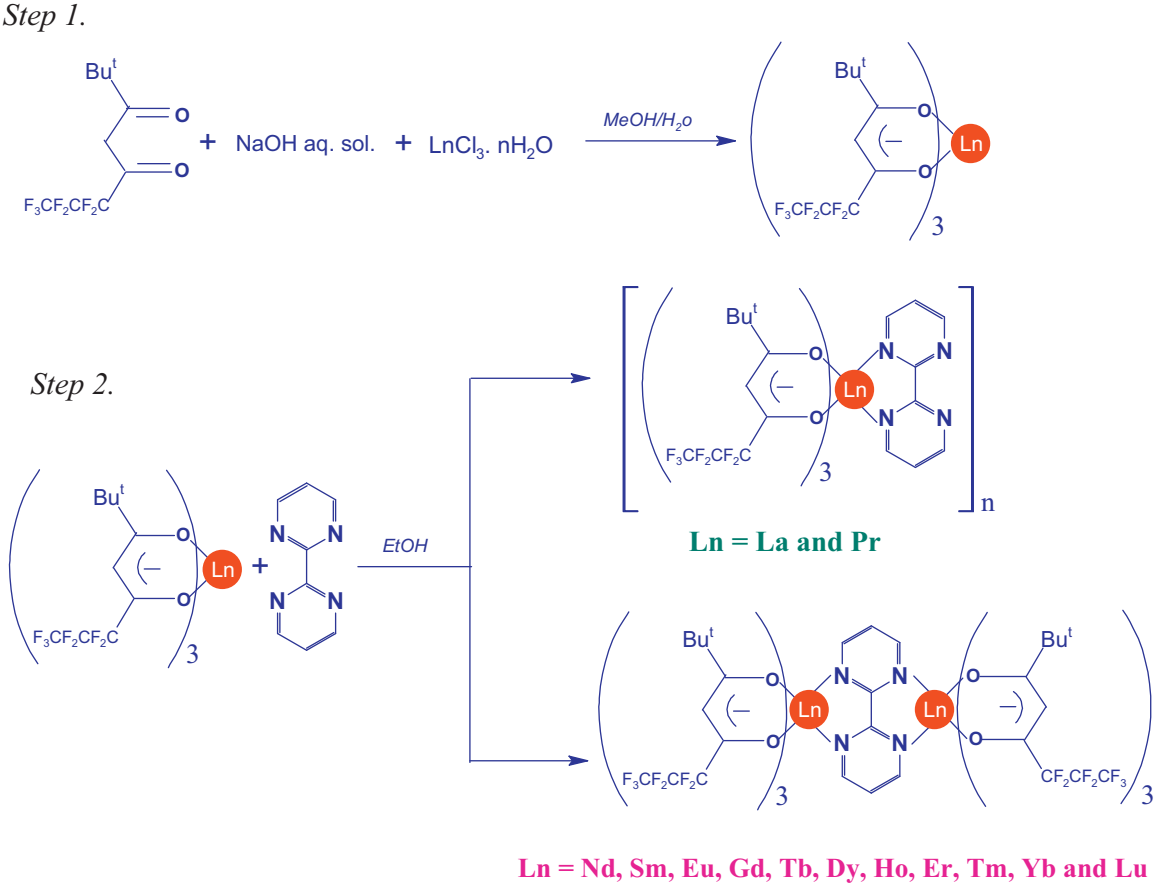

Scheme 1. Synthesis of the complexes.

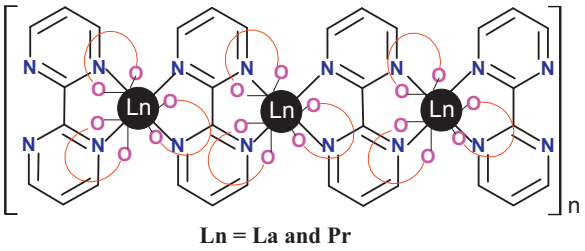

Chart 1. Representation of one dimensional coordination array structure of La and Pr complexes. Red semicircles attached with pink O–atoms at the ends represent the fod units attached to Ln(III) ion. (For interpretation of the references to colour in this figure legend, the reader is referred to the web version of this article.)

anion of 2-thenoyltrifluoroacetone) where X-ray crystal structure of this complex has shown that it adopts a polymeric array of the type $[Nd(tta)_3(bpm)]_n$ and by one-dimensional structure for the analogous bpm-bridged complexes [33,34]. It is, therefore, concluded that La(III) and Pr(III) complexes are ten-coordinate in a polymeric array in which each metal ion is coordinated to three fod ligands and two NN donors from two bpm units as represented in Chart 1. This is in contrast to the eight-coordinate dinuclear complexes formed by the rest of the lanthanides (Nd–Lu). The reasons for the unusual reactivity shown by La(III) and Pr(III) chelates are likely the large size of these metal ions which are capable of achieving higher coordination than the rest of the lanthanide ions and the lower basicity of bpm ($pK_a = 0.6$) which would facilitate these larger tripositive lanthanide ions to coordinate with two NN donors of bpm instead of one NN donor to attain greater electron affluence. The ten-coordinate complexes with lanthanum and praseodymium have been recently reported with hexafluoroacetylacetone (hfaa) and phenanthroline [13,15].

3.3. ES^+–MS

Electrospray mass spectra of all the complexes in positive ion mode were recorded in chloroform. None of the complexes displays intact molecular ion peak. The various lanthanide containing peaks observed on the mass spectra could not be assigned by the general rules of fragmentation of lanthanide β-diketonates, possibly due to fragmentation of fod moieties. The mass spectra of the fluorinated β-diketonate complexes are complicated due to easy splitting of CF_3 fragments and by the possibility of migration of the F atoms [35]. However, the peaks representing mononuclear fragments $[Ln(fod)_2(bpm)]^+$ and $[Ln(fod)_2(bpm)_2]^+$ are easily assigned for all the complexes. The $[Ln(fod)_2(bpm)_2]^+$ fragment of Er and Tm complexes are observed with 100% abundance (Figs. S1 and S2 in Supporting information). None of the spectra displayed the peak for the fod^+ ion which strengthens the idea for the partial fragmentation of fod moieties.

3.4. Thermal studies

The thermograms of the complexes were studied under a N_2 atmosphere at a heating rate of 10 °C/min. The complexes exhibit similar thermal behaviour which is consistent with the one step evaporation. The TGA/DTA plots of some representative complexes are given in Fig. 1. The complexes are thermally stable and melting points of the dinuclear complexes are in the range between 203 and 230 °C (Nd–Lu) with increasing trend across the lanthanide series. These melting points are much higher than the mononuclear $[Ln(fod)_3(bpy)]$ and $[Ln(fod)_3(phen)]$ analogues [13] which reflects that these dinuclear complexes are thermally more stable than their mononuclear phen and bpy analogues. However, it is interesting to point out that the melting point of the polymeric

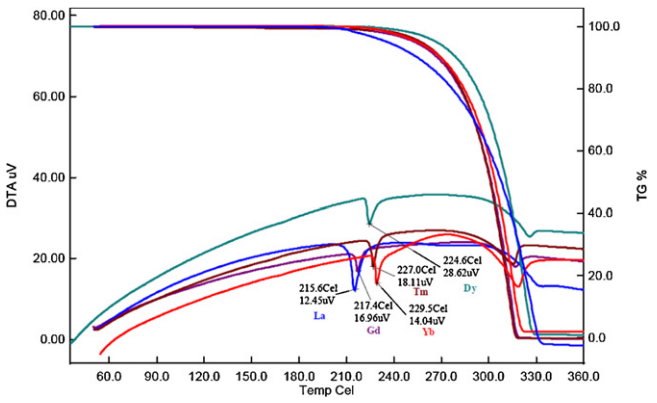

Fig. 1. TGA/DTA plot of representative new complexes.

praseodymium complex (mp = 161 °C) is lower that the melting point of the polymeric lanthanum complex (mp = 215 °C), although the radius of the La(III) ion (~121.6 pm) is larger than the radius of Pr(III) ion (~117.9 pm). This could be related to the larger steric crowding around the smaller Pr(III) ion due to ten-coordinated polymeric structure. Since the radius of the La(III) ion is larger, lesser steric congestion is expected and hence higher melting point. It may be emphasized that the steric crowding has a strong influence on the thermal stability of the complexes. The DTA curve of the complexes shows two endothermic peaks; one sharp lower temperature peak corresponds to the melting of the complex and the other peak at higher temperature is consistent with the volatilization. The volatile nature and improved stability of these complexes over their mononuclear analogues makes them very good candidate to form luminescent thin films for their possible use in electroluminescent devices.

4. ^{1}H NMR studies

4.1. Diamagnetic La(III) and Lu(III) complexes

The ^{1}H NMR spectra of lanthanum and lutetium complexes in $CDCl_3$ gave an insight into the solution structure of these complexes. The ^{1}H NMR spectrum of the lanthanum complex (Fig. 2) exhibits only one set of signals for the bipyrimidine and diketonate moiety, suggesting that a single species exists in the solution. The signals observed are assigned to *tert*-butyl (0.92 ppm); methine (5.79 ppm) protons of the fod moiety and H-2/H-2′ (9.28 ppm) and H-3 (7.55 ppm) protons of the coordinated bpm in the intensity ratio of 27:3:4:2, respectively. The H-2/H-2′ and H-3 proton resonances are shifted to downfield, as compared to their position in free bpm (Table 1) and these shifts are consistent with the ligand binding to the metal ion. The magnitude of the diamagnetic shift is smaller for the lanthanum complex (e.g. 0.25 ppm (δ) for H-2) than the lutetium complex (0.48 ppm for H-2) (Table 1) [20]. The larger downfield shift of bpm protons in the lutetium complex is related to the smaller size and greater electropositive charge density on

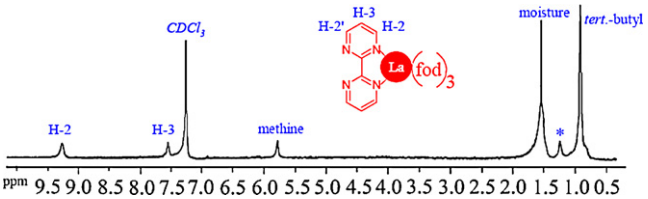

Fig. 2. 300 MHz ^{1}H NMR spectrum of $[La(fod)_3(bpm)]_n$ in $CDCl_3$. * represents some impurity.

Table 1
The chemical shifts (δ) and paramagnetic shifts ($\Delta\delta$) of dinuclear lanthanide complexes $[Ln_2(fod)_6(\mu\text{-bpm})]$ and their precursor $Ln(fod)_3$ chelates.

Compound	δH-2/Δδ(H-2)	δH-3/Δδ(H-3)	δCH/Δδ(CH)	δBu^t/Δδ(Bu^t)
2,2′-Bipyrimidine	9.03, t	7.45, d	–	–
$[La(fod)_3(bpm)]_n$	9.28	7.55	5.79	0.93
$La(fod)_3$	–	–	5.94	1.09
$[Lu_2(fod)_6(\mu\text{-bpm})]$	9.46, t	7.72, d	5.83	0.96
$Lu(fod)_3$	–	–	6.05	1.10
$[Pr(fod)_3(bpm)]_n$	−26.50 (−35.78)	−2.10 (−9.65)	21.71 (15.92)	1.25 (0.32)
$Pr(fod)_3$	–	–	19.6	0.35
$[Nd_2(fod)_6(\mu\text{-bpm})]$	−0.79 (−10.28)	2.16 (−5.39)	11.36 (5.57)	0.68 (−0.25)
$Nd(fod)_3$	–	–	11.83	0.95
$[Sm_2(fod)_6(\mu\text{-bpm})]$	8.52 (−0.76)	7.15 (0.40)	7.02 (1.23)	0.88 (−0.05)
$Sm(fod)_3$	–	–	7.50	1.07
$[Eu_2(fod)_6(\mu\text{-bpm})]$	13.56 (4.28)	12.02 (4.47)	2.64 (−3.15)	1.82 (0.89)
$Eu(fod)_3$	–	–	23.14	1.56
$[Tb_2(fod)_6(\mu\text{-bpm})]$	[a]	[a]	124.65 (118.82)	−3.17 (−4.13)
$Tb(fod)_3$	–	–	–	−7.61
$[Dy_2(fod)_6(\mu\text{-bpm})]$	[a]	[a]	[a]	−13.66 (−14.62)
$Dy(fod)_3$	–	–	[a]	−13.45
$[Ho_2(fod)_6(\mu\text{-bpm})]$	[a]	[a]	69.73 (63.90)	−4.31 (−5.27)
$Ho(fod)_3$	–	–	79.07	−8.98
$[Er_2(fod)_6(\mu\text{-bpm})]$	39.10 (29.64)	31.47 (23.75)	−19.43 (−25.26)	6.32 (5.36)
$Er(fod)_3$	–	–	−24.46	1.19
$[Tm_2(fod)_6(\mu\text{-bpm})]$	[a]	[a]	−34.12 (39.95)	6.53 (5.57)
$Tm(fod)_3$	–	–	−70.41	6.42
$[Yb_2(fod)_6(\mu\text{-bpm})]$	12.21 (2.75)	21.94 (14.22)	−10.19 (−16.02)	5.17 (4.21)
$Yb(fod)_3$	–	–	−19.66	4.59

The paramagnetic shifts ($\Delta\delta$) of the complexes are calculated as the deviation of chemical shift (δ) in paramagnetic Pr–Eu complexes from that of diamagnetic La complex and paramagnetic Tb–Yb complexes from diamagnetic Lu complex.

[a] These resonances are broadened beyond detection.

the Lu(III) ion than the La(III) ion which results in more deshielding of the bpm protons.

The lanthanum complex (Fig. 2) was expected to display three signals for the coordinated bpm in the intensity ratio of 1:1:1 for H-2, H-2′ and H-3 protons. However, the NMR spectrum displays only two resonances for bpm protons with the area under the peak in 1:2 ratio. This reflects that H-2 and H-2′ protons are equivalent. It is only possible if all four nitrogen atoms of bpm are coordinated to lanthanum. It leads towards existence of a dinuclear species but the elemental analysis gives a mononuclear complex of the type $[La(fod)_3(bpm)]$. Therefore, only way to explain its structure is to consider a long polymeric chain of repeating $[Ln(fod)_3(bpm)]$ units as shown in Chart 1. This corroborates with the IR result and gets support from the literature on similar lanthanide complexes [22,33,34] (*vide supra*).

The *tert*-butyl and methine resonances of both lanthanum and lutetium complexes are shifted to upfield as compared to their positions in $La(fod)_3$ and $Lu(fod)_3$ chelates, respectively (Table 1). The shielding of these resonances occurs because after withdrawing the electron density from N donors of the bipyrimidine, the Ln(III) ion becomes more polarized and transfers some charge *via* the π system of the diketonate ring and this can be very conveniently accommodated by the fluorine atoms (due to their large electronegativity).

4.2. Paramagnetic complexes

The NMR spectra of all the paramagnetic complexes and their parent chelates are recorded in $CDCl_3$ and the representative spectra of Nd and Eu complexes are shown in Figs. 3 and 4, respectively. The chemical shifts, δ (ppm) and paramagnetic shifts, $\Delta\delta$ (ppm) are given in Table 1. The spectra are the first order and assignments are based on relative intensities and comparison with their parent chelates. More structural information may be obtained from the analysis of moderate to huge paramagnetic shifts, observed for these complexes. The paramagnetic shifts in case of trivalent lanthanides are predominantly dipolar (pseudo-contact) in nature since the radial extension of 4f orbitals is exceedingly small and the electrons in the 4f-orbitals are shielded from the ligands by 5s and 5p electrons. These paramagnetic shifts arise from a through-space dipolar interaction between the electronic magnetic moment and the nuclear magnetic moment of the resonating diamagnetic ligand (bpm and fod) nuclei, which does not vanish for magnetically anisotropic systems. As a consequence of this dipolar-interaction the resonances of fod and bpm protons are markedly shifted from the position observed in the corresponding diamagnetic lanthanum

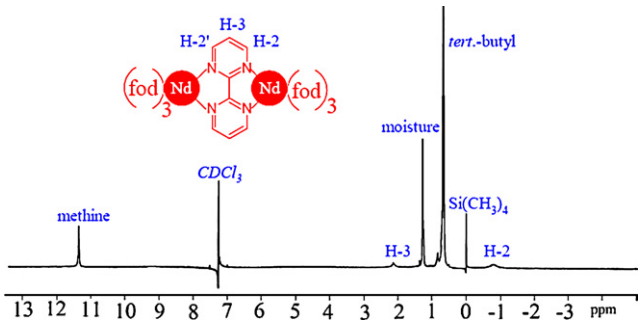

Fig. 3. 400 MHz ^{1}H NMR spectrum of $[Nd_2(fod)_6(\mu\text{-bpm})]$ in $CDCl_3$.

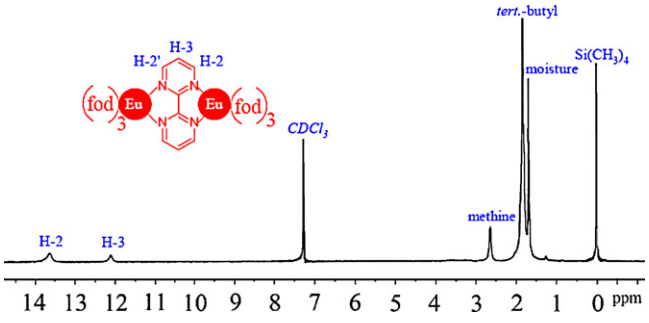

Fig. 4. 400 MHz ^{1}H NMR spectrum of $[Eu_2(fod)_6(\mu\text{-bpm})]$ in $CDCl_3$.

or lutetium complex. The paramagnetic shifts (arising out of dipolar mechanism) provide information relating to the geometrical configuration of the ligands about a metal ion in solution and are limited by the geometry of the complex species. The following features of the spectra of the complexes investigated are obvious:

i Only one set of signals is observed for the aromatic as well as β-diketonate protons which substantiates the presence of only one species in the solution.
ii The spectra of the complexes generally display four resonances; one each due to *tert*-butyl, methine, H-2 and H-3 protons in the intensity ratio of 54:6:4:2, respectively (indicating that the β-diketonate to bpm ratio, in the complexes, is 6:1). This substantiates the presence of intact dinuclear species present in the solution.
iii The spectra of the complexes show sizable downfield shifts in Eu, Er, Tm and Yb complexes or upfield shifts in Pr, Nd, Tb, Dy and Ho complexes for bpm and *tert*-butyl resonances. The Sm complex shows very small upfield shifts for these protons and the spectrum is comparable with the diamagnetic analogues.
iv The room temperature paramagnetic shift obtained for methine protons of the β-diketone moiety has the opposite sign with respect to that of paramagnetic shifts of aromatic and *tert*-butyl protons.
v The bpm resonances could not be observed for Tb, Dy, Ho and Tm complexes even in the 200 to −200 ppm range. It could be due to much higher magnetic moment of these metal ions leading to paramagnetically enhanced relaxation of the nuclei which broadens the lines beyond detection limits.
vi No change in signal line width or position is seen on keeping the solutions for few days. This proves that both the ends of both bpm and fod remain coordinated in solution and there is no dissociation of any of the ligands present.

4.3. Relative shifting

For all the complexes studied the changes produced in the chemical shift of bpm protons is a function of the central atom which can be related to the magnetic anisotropy of the lanthanide(III) ion. Among early lanthanides, relatively large upfield shifts are noted for praseodymium complex then becoming very small for samarium with the change in the sign at europium which causes downfield shifts of slightly smaller magnitude. It is to be mentioned for Pr, Nd and Sm complexes that the upfield paramagnetic shift is larger for H-2 protons than H-3, reflecting the fact that the paramagnetic shift decreases with increasing distance of the proton from the metal. However, in the case of europium complex, the paramagnetic shift is slightly larger for H-3 protons as compared to H-2 protons (Table 1). Sizable down field displacements of bpm resonances are noted for Er and Yb complexes with the largest one for erbium. It is to be pointed out that the chemical shifts of the bpm protons induced by the various metal ions in these complexes are uniformly directed, i.e. the paramagnetic shift is larger for H-2 protons as compared to H-3 protons. However, as found in the case of [Yb(hfaa)$_3$(phen)] [14], the paramagnetic shifts of H-2 and H-3 protons of bpm in the case of [Yb$_2$(fod)$_6$(μ-bpm)] complex is not uniformly directed. In spite of being closer to Yb the H-2 protons are much less displaced than H-3 protons and appear at higher field than H-3.

The paramagnetic shift of the *tert*-butyl resonance of the fod moieties followed the similar trend as observed for bpm protons. However, the Pr complex is an exception where this resonance is shifted to downfield despite Pr being an upfield shifter. The *tert*-butyl resonance is slightly shifted to upfield in the case of Nd and Sm complexes. The triad Tb, Dy and Ho are known upfield shifters, so the *tert*-butyl resonance of these complexes is significantly upfield shifted. The triad Er, Tm and Yb (known down field shifters) shift this resonance to down field.

The opposite direction shift of the methine resonance of these complexes reflects importance of the geometric factor $3\cos^2\theta - 1$, in changing the sign of the shift. Therefore, it seems likely that the average geometric factor of the aromatic and the methine protons have opposite sign and the paramagnetic shift is exclusively due to dipolar interaction. This gets support from our earlier observations [13,36] and observation noted on Ln(C$_5$H$_5$)$_3$B (where B is an uncharged aprotic Lewis base), where the signal positions of the ligand B have their sign opposed to that of ring protons [37].

The direction and magnitude of the paramagnetic shifts observed for dinuclear complexes (Table 1) are comparable to the mononuclear analogous with [Ln(fod)$_3$(bpy)] and [Ln(fod)$_3$(phen)] [36]. This indicates that the two Ln sites in the dinuclear complexes are independent of each other and behave as isolated centers and the interaction between two paramagnetic Ln centers is negligible for the interpretation of ^{1}H NMR spectra. This is supported by the work of Ishikawa et al. [38] who observed that paramagnetic shifts in the Ln(III)–Ln(III) complexes are independent of the presence of two Ln centers due the negligible interaction between them and observed magnetic moment of these complexes.

A comparison of the NMR resonances of fod moieties (*tert*-butyl and methine) in dinuclear complexes is made with their parent Ln(fod)$_3$ chelates (Table 1). The chemical shifts of these protons in the complexes are different from their chemical shifts in the chelates. This variation of the chemical shifts in the complexes as compared to their chelates is attributed to the change in the geometry around Ln(III) ion after the coordination with bpm.

4.4. Line broadening

The extent of line broadening is essentially a function only of the lanthanide ion. The signal line broadening of the protons near a paramagnetic lanthanide ion is governed by both the dipolar interaction and Curie-spin relaxation; and the line width depends upon the magnetic field and the inverse sixth power of the corresponding proton lanthanide distance [39,40]. The difference in relative broadening reflects different metal proton distances, the broader peaks being associated with the proton nuclei of the ligands closer to the lanthanides. We first discuss the effect of line broadening on bpm resonances because of their proximity to the metal ions and the absence of spin–spin splitting. We observed that the bpm resonances are broad in the present dinuclear complexes as compared to resonances of aromatic amines in the mononuclear complexes [Ln(fod)$_3$(phen)] and [Ln(fod)$_3$(bpy)] [13,36]. Of the early lanthanides the Sm and Eu causes least signal broadening while the bpm resonances of Nd complex are relatively broader. In the case of Pr complex, very broad resonance are observed for H-2 protons while the H-3 resonance is observed with lesser broadening. The bpm resonances observed in Yb and Er complexes are severely broadened. As already mentioned, the resonances due to bpm protons of Tb, Dy, Ho and Tm complexes were not observed at all. It is important to mention that the resonances due to aromatic heterocyclic ligands in cases of heavy lanthanide (Tb, Dy, Ho and Tm) in mononuclear complexes [Ln(fod)$_3$(phen)], [Ln(fod)$_3$(bpy)] and [Ln(hfaa)$_3$(phen)] are observed, except H-2 protons in Dy complexes. Furthermore, the *tert*-butyl resonance of the heavy lanthanide dinuclear complexes is much broader than this resonance in the corresponding chelate. This resonance is very sharp in the chelate (Fig. S3 in Supporting information). Therefore, it is concluded that the severe line broadening in the dinuclear complexes is possibly due to the presence of two paramagnetic Ln(III) ions which lead to much enhanced relaxation of the nuclei.

4.5. Shift ratios

The intramolecular shift ratios, R_{ij} of the shift of the nucleus i to another j in an isomorphous series of the complexes remain the same for all the lanthanides, if the shift is dipolar in nature and should reveal stereochemical arrangement of protons with respect to the central ion and principal axis of the complex [13,36,41]. Among the complexes where bpm resonances are detected (Pr, Nd, Sm, Eu, Er and Yb) we observe that the intra-molecular chemical shift ratios of H-2 and H-3 protons of only dinuclear Sm, Eu, and Er complexes are constant, i.e. ~1.2. This favours that these complexes have similar geometry in solution, the geometric factors are fairly fixed for these three complexes and shifts are predominantly pseudocontact in origin. We also compare intermolecular shift ratios of H-2 and H-3 protons of these complexes; for example H-2(Sm)/H-2(Eu) = 0.62 and H-3(Sm)/H-3(Eu) = 0.60; H-2(Sm)/H-2(Er) = 0.21 and H-3(Sm)/H-3(Er) = 0.22; H-2(Eu)/H-2(Er) = 0.34 and H-3(Eu)/H-3(Er) = 0.38, and found that ratios are fairly constant which strongly support that shifts are dipolar in origin and the three complexes have fixed geometric factors and adopt similar structure in the solution. However, the chemical shift ratios for Pr, Nd and Yb complexes are not constant. This may be either due to a different geometry adopted by these complexes in solution or some contact contribution to the paramagnetic shift. The intramolecular chemical shift ratio of H-2 and H-3 protons of bpm, calculated from the ^{1}H NMR data of $[Eu_2(nta)_6(\mu\text{-bpm})]$ [42] {nta is the anion of 1-(2-naphthoyl)-3,3,3-trifluoroacetone} is also ~1.2. The X-ray structure of this complex has been reported to be distorted square antiprismatic. Therefore, distorted square antiprismatic structure may be predicted for the Sm, Eu and Er complexes since the chemical shift ratios for the H-2 and H-3 protons of these complexes are similar to $[Eu_2(nta)_6(\mu\text{-bpm})]$ [42]. This geometry is common for bipyrimidine-bridged lanthanide tris β-diketonate complex reported in the literature [21–23].

5. Photoluminescence properties

The steady state luminescence properties of the Pr(III), Sm(III), Eu(III), Tb(III) and Dy(III) complexes at equimolar concentration were investigated in chloroform solution. The excitation spectra of the complexes (Fig. S4 in Supporting information) display a broad band (330–420 nm) with maxima at 349, 355, 362, 356 and 357 nm for Pr(III), Sm(III), Eu(III), Tb(III) and Dy(III) complexes, respectively. These bands correspond to the excitation of the organic ligands ($S_0 \rightarrow S_1$). The excitation spectra of the complexes show a good overlap with the ligand centered π–π^* absorption bands (240–410 nm) of the complexes in chloroform. This confirms that an energy transfer takes place from the ligands to the Ln(III) ion (*antenna effect*). The excitation spectra of the complexes were recorded by monitoring the most intense f–f emission transition of the given complex. The luminescence spectra of the complexes were recorded by selecting the excitation wavelength at $S_0 \rightarrow S_1$ band maxima to get the maximum intensity.

The emission spectrum of $[Sm_2(fod)_6(\mu\text{-bpm})]$ in chloroform is shown in Fig. 5. The complex exhibits intense characteristic emission of Sm(III) ion upon excitation with a wavelength of 355 nm. The three peaks are assigned to (i) $^4G_{5/2} \rightarrow {}^6H_{5/2}$ (564 nm); (ii) $^4G_{5/2} \rightarrow {}^6H_{7/2}$ (605 nm) and (iii) $^4G_{5/2} \rightarrow {}^6H_{9/2}$ (646 nm) transitions of Sm(III). The $^4G_{5/2} \rightarrow {}^6H_{9/2}$ is an electric-dipole hypersensitive transition. The $^4G_{5/2} \rightarrow {}^6H_{5/2}$ transition has a predominant magnetic-dipole character. The hypersensitive transition is most intense in the spectrum followed by $^4G_{5/2} \rightarrow {}^6H_{7/2}$ transition. The $^4G_{5/2} \rightarrow {}^6H_{7/2}$ transition shows three stark components at 600, 605 and 610 nm. The high intensity of the hypersensitive transition and stark splitting in $^4G_{5/2} \rightarrow {}^6H_{7/2}$ indicates a low symmetry

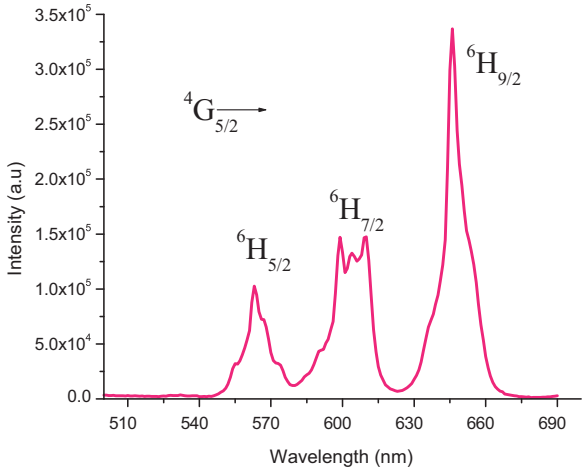

Fig. 5. Emission spectrum of $[Sm_2(fod)_6(\mu\text{-bpm})]$ in chloroform.

coordination around Sm(III) centers in the dinuclear complex [43]. The emission spectrum of $[Eu_2(fod)_6(\mu\text{-bpm})]$ (Fig. 6) displays transitions originating from the $^5D_0$ emitting state of Eu(III) to ^7F_j (j = 0, 1, 2, 3, and 4) manifolds. The most intense transition in the emission spectrum of the complex is the induced electric-dipole, $^5D_0 \rightarrow {}^7F_2$ hypersensitive transition. This transition is notably much more intense than the magnetic-dipole, $^5D_0 \rightarrow {}^7F_1$ transition, which reflects a low symmetry of the Eu(III) site. Furthermore, the emission spectrum of the complex shows only one peak for the $^5D_0 \rightarrow {}^7F_0$ transition indicating the presence of a single chemical environment around the Eu(III) ion. The $[Tb_2(fod)_6(\mu\text{-bpm})]$ complex (Fig. 7) displays transitions originating from the $^5D_4$ emitting state of Tb(III) to ^7F_j (j = 6, 5, 4, and 3) manifolds. The spectrum is dominated by the $^5D_4 \rightarrow {}^7F_5$ transition at 543 nm which is responsible for the green luminescence of this complex. The $^5D_4 \rightarrow {}^7F_4$ and $^5D_4 \rightarrow {}^7F_3$ transitions have weak intensities as compared to other two transitions in the spectrum and display stark splitting. Both transitions are sensitive to the coordination and the stark splitting is indicative of a very low symmetry around Tb(III) centers in the complex [44]. The $[Dy_2(fod)_6(\mu\text{-bpm})]$ complex (Fig. 8) consists of three transitions due to the deactivation of $^4F_{9/2}$ emission level to the lower energy levels. These are assigned to (i) $^4F_{9/2} \rightarrow {}^6H_{15/2}$ (482 nm), (ii) $^4F_{9/2} \rightarrow {}^6H_{13/2}$ (573 nm) and (iii) $^4F_{9/2} \rightarrow {}^6H_{11/2}$ (659 nm) transitions of Dy(III). The $^4F_{9/2} \rightarrow {}^6H_{15/2}$ transition is magnetically allowed and does not vary with the local field around the Dy(III) ion, however $^4F_{9/2} \rightarrow {}^6H_{13/2}$ is a forced

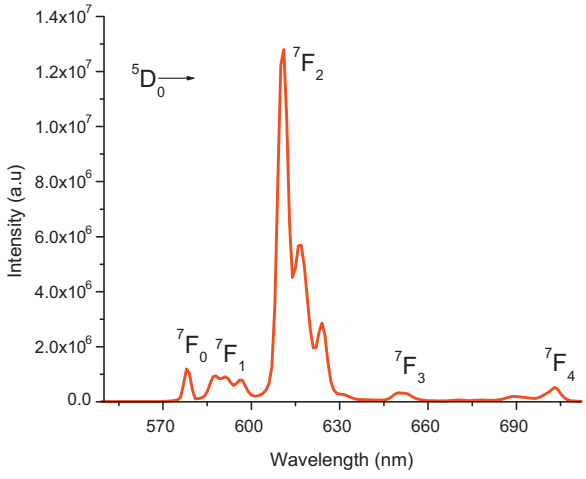

Fig. 6. Emission spectrum of $[Eu_2(fod)_6(\mu\text{-bpm})]$ in chloroform.

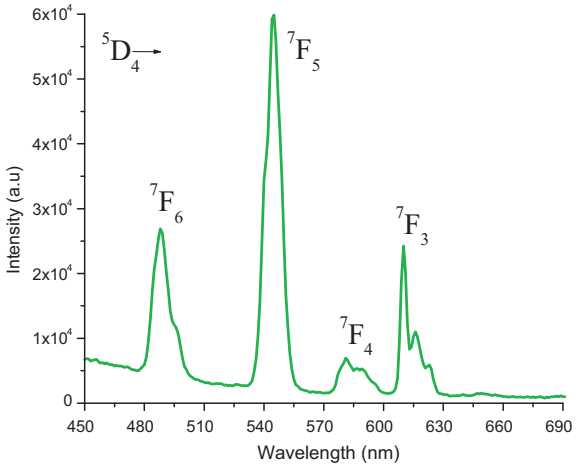

Fig. 7. Emission spectrum of $[Tb_2(fod)_6(\mu\text{-bpm})]$ in chloroform.

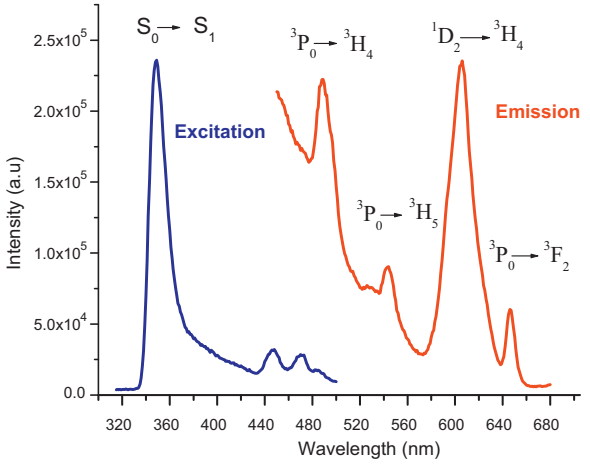

Fig. 9. Excitation and emission spectra of $[Pr(fod)_3(bpm)]_n$ in chloroform.

electric-dipole transition and is most intense transition in the emission spectrum. It may be emphasized that the $^4F_{9/2} \rightarrow {}^6H_{13/2}$ transition is prominent only when the Dy(III) ion is located at a low symmetry site which allows the intensification of this transition. Therefore, this transition is used as a probe for the site symmetry in Dy(III) systems [45].

The red and green luminescence of Eu(III) and Tb(III) complexes, respectively, and to a lesser extent the pink and yellow luminescence of Sm(III) and Dy(III) complexes, respectively, have been thoroughly investigated and these complexes are exploited in electroluminescent devices and many other applications [1–8,10]. In contrast, reports on the emission spectrum of the Pr(III) complexes is scarce [13,46–48]. The excitation and emission spectra of $[Pr(fod)_3(bpm)]_n$ are shown in Fig. 9. The emission spectrum displays a series of transitions in the visible region. The most intense peak centered at 605 nm is assigned to $^1D_2 \rightarrow {}^3H_4$ hypersensitive transition. This transition is also believed to be overlapped by a much weaker $^3P_0 \rightarrow {}^3H_6$ transition [47]. The other emission bands correspond to the $^3P_0 \rightarrow {}^3H_4$ (488 nm), $^3P_0 \rightarrow {}^3H_5$ (543 nm) and $^3P_0 \rightarrow {}^3F_2$ (646 nm) transitions. It is interesting to note that the emission spectrum of the Pr complex displays transitions from two different excited levels (i.e. $^3P_0$ and $^1D_2$) to three different manifolds (i.e. $^3H_4$, $^3H_5$ and $^3F_2$).

A comparison of the luminescence intensity of the Sm(III), Eu(III), Tb(III), Dy(III) and Pr(III) complexes gives the following order: Eu(III) ⋙ Sm(III) > Pr(III) > Tb(III) ≈ Dy(III) (Table 2). The

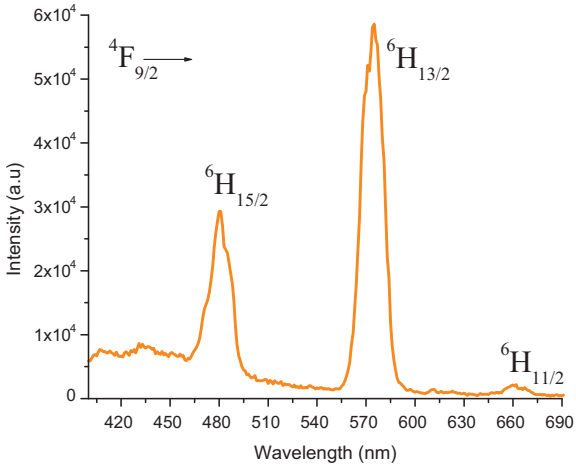

Fig. 8. Emission spectrum of $[Dy_2(fod)_6(\mu\text{-bpm})]$ in chloroform.

$^5D_0 \rightarrow {}^7F_2$ hypersensitive transition of Eu(III) complex is 38 times more intense than the $^4G_{5/2} \rightarrow {}^6H_{9/2}$ hypersensitive transition of Sm(III) and 54 times more intense than the $^1D_2 \rightarrow {}^3H_4$ hypersensitive transition of Pr(III). It is noteworthy that this transition of Eu(III) is 213 and 218 times more intense than the most intense $^5D_4 \rightarrow {}^7F_5$ transition of Tb(III) and $^4F_{9/2} \rightarrow {}^6H_{13/2}$ transition of Dy(III) complex, respectively. These results indicate that the energy transfer from the organic ligands (fod and bpm) to Eu(III) is most efficient followed by the energy transfer to Sm(III) and Pr(III) while inefficient or partial energy transfer takes place from antenna ligands to Dy(III) and Tb(III). The weaker luminescence of the Tb(III) complex than Sm(III) and Pr(III) complexes is surprising. It is well documented [3,10] that Pr(III), Sm(III) and Dy(III) complexes have inherent weaker luminescence intensity as compared to Eu(III) and Tb(III) complexes. It is due to the smaller energy gap between the emitting level and the next lower energy level: *ca.* ~7400 cm^{-1} for Sm(III); ~7850 cm^{-1} for Dy(III) and ~6940 cm^{-1} for Pr(III) versus *ca.* ~12,300 cm^{-1} for Eu(III) and ~14,800 cm^{-1} for Tb(III) [49–51]. The smaller energy gap results in a more efficient quenching of the excited states in the case of Pr(III), Sm(III) and Dy(III) ions.

However, it is a well known fact that the luminescence efficiency of the lanthanide complexes also depends upon the effective match between the emitting level of the Ln(III) ion and ligand centered triplet state [52]. There are two types of ligands attached to the Ln(III) ions in these complexes with different energy of the triplet states. The energy level of the fod centered triplet level lies around 22,500 cm^{-1} [26] while the bpm centered triplet level has been estimated around 24,100 cm^{-1} [22,53]. These triplet energy levels are well above the main emitting levels of Sm(III) $\{^4G_{5/2}$, ~17,900 $cm^{-1}\}$, Eu(III) $\{^5D_0$, ~17,280 $cm^{-1}\}$, Dy(III) $\{^4F_{9/2}$,~21,100 $cm^{-1}\}$, Tb(III) $\{^5D_4$, ~20,500 $cm^{-1}\}$ and Pr(III) $\{^1D_2$, ~16,840 $cm^{-1}\}$ (Fig. 10) [49–51]. The energy difference between the fod centered triplet level and the emitting levels of Ln(III) ions is approximately 4600, 5220, 1400, 2000 and 5660 cm^{-1} for Sm(III), Eu(III), Dy(III), Tb(III) and Pr(III) ions, respectively, while energy difference between the bpm centered triplet level and emitting levels of Ln(III) is approximately 6200, 6820, 3000, 3600, and 7260 cm^{-1}

Table 2
Emission intensity of the most intense transitions of the complexes.

Complex	Transition	Energy (nm)	Intensity (a.u.)
Eu	$^5D_0 \rightarrow {}^7F_2$	612	12,886,825
Sm	$^4G_{5/2} \rightarrow {}^6H_{9/2}$	646	339,030
Pr	$^1D_2 \rightarrow {}^3H_4$	605	237,014
Tb	$^5D_4 \rightarrow {}^7F_5$	545	60,426
Dy	$^4F_{9/2} \rightarrow {}^6H_{13/2}$	573	58,955

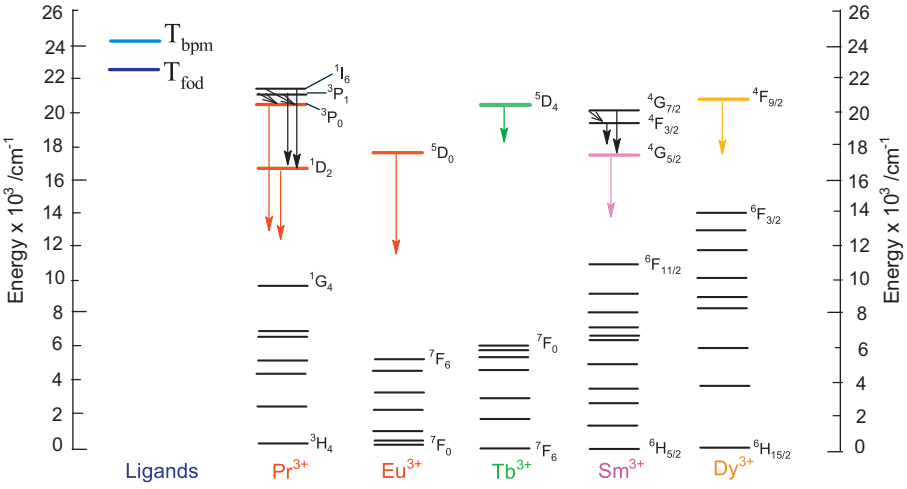

Fig. 10. Simplified energy diagram showing lanthanide excited states and their position with respect to the triplet states of fod and bpm sensitizers.

for Sm(III), Eu(III), Dy(III), Tb(III) and Pr(III) ions, respectively. It has been reported that an optimal ligand-to-metal energy transfer process for Tb(III) needs Δ_E ($^3\pi\pi^* - {}^5D_4$) = 2500–4500 cm^{-1} [52]. Therefore, these investigations point out that the triplet level of the main sensitizer (fod) is too close to the emitting level of Tb(III) which should lead to the efficient back energy transfer from Tb(III) emitting level to triplet level of fod [52].

The inefficient sensitization by the fod ligand to the Tb(III) luminescence is confirmed by the weak emission observed from the spectrum of Tb(fod)$_3$ chelate in chloroform upon excitation at 350 nm within a π–π^* transition of fod. Since the triplet level of bpm ligand matches well with the $^5D_4$ emitting level of Tb(III) (Δ_E = 3000 cm^{-1}) [52] and emission of the dinuclear complex is enhanced as compared to the emission of Tb(fod)$_3$ chelate, it confirms that the Tb(III) emission of [Tb$_2$(fod)$_6$(μ-bpm)] is primarily sensitized by bpm. Elsewhere, bpm has been reported to be very efficient sensitizer for the Tb(III) luminescence [53]. The very low intensity of the Tb(III) emission as compared to the Eu(III) emission could be related to the presence of single bpm sensitizer attached to two Tb(III) ions in the terbium complex while there are three units of fod sensitizers attached to each Eu(III) ion in addition to a bridging bpm unit which also acts as sensitizer in the case of europium complex. Furthermore, the lower intensity of Tb(III) emission in the present complex could also be related to the loss of energy due to interligand energy transfer [22]. It is postulated that upon excitation of the singlet state of bpm, part of the energy is absorbed by the excited states of fod since their position lies lower than the excited states of bpm. Subsequently, from the populated excited states of bpm, part of the energy is transferred to the excited states of fod. Since fod is inefficient in transferring this energy to the $^5D_4$ emitting level, the Tb(III) ions receive lesser energy than expected from the bpm ligand.

The strongest emission intensity noted for the Eu(III) complex is not surprising since the energy difference between the triplet levels of the ligands (fod and bpm) and the emitting level of Eu(III) is optimum [52–54] and energy transfer originates from both the ligands and results in largest luminescence.

The bright luminescence of the Sm(III) complex also reflects an efficient energy transfer from both fod and bpm centered triplet levels and $^4G_{5/2}$ emitting level of this metal ion possibly due to a good energy match. In fact, the excitation of Sm(fod)$_3$ around 350 nm in chloroform gives characteristic Sm(III) emission and the intensity of this emission is further enhanced many times upon its coordination to bpm [29]. These results confirm that both fod and bpm are good ligands for the sensitization of Sm(III) emission. Furthermore, it was recently shown that bpm could sensitize Sm(III) emission which was relatively more intense in [Sm(NO$_3$)$_3$(bpm)$_2$] having two bpm molecules in the first coordination sphere, than in the [Sm(NO$_3$)$_3$(bpm)(CD$_3$OD)$_2$] which contains only one bpm molecule [53].

Although the characteristic emission of Sm(III) is observed from the $^4G_{5/2}$ level, there are two more excited states for the Sm(III) ion lying very close to this level. These are $^4G_{7/2}$ (~20,050 cm^{-1}) and $^4F_{3/2}$ (~18,900 cm^{-1}) (Fig. 10). The energy difference between the triplet state of fod and $^4G_{7/2}$ and $^4F_{3/2}$ excited levels of Sm(III) are ~2450 cm^{-1} and ~3600 cm^{-1}, respectively, while the energy difference between the triplet state of bpm and $^4G_{7/2}$ and $^4F_{3/2}$ excited levels of Sm(III) are ~4050 cm^{-1} and ~5200 cm^{-1}, respectively. These energy differences between triplet levels of the ligands and $^4G_{7/2}$ and/or $^4F_{3/2}$ levels are lower than the difference between $^4G_{5/2}$ and fod and/or bpm levels. It is, therefore, postulated that the energy transfer to the $^4G_{5/2}$ emitting level of Sm(III) ion occurs *via* population of these higher energy ($^4G_{7/2}$ and $^4F_{3/2}$) states and subsequent relaxation to the $^4G_{5/2}$ emitting level. Therefore, the bright emission of Sm(III) comes from $^4G_{5/2}$ level. The fact that a very weak emission transition, $^4F_{3/2} \rightarrow {}^6H_{5/2}$ is noted at 537 nm further strengthens the contention that the energy transfer occurs *via* population of higher energy states.

The Dy(III) emission is not thoroughly investigated and therefore, no definite data are available regarding optimum energy gap between the triplet state of the antenna ligand and $^4F_{9/2}$ emitting level of Dy(III) ion for an efficient energy transfer [55]. We find that fod is an inefficient ligand for the sensitization of dysprosium emission since its triplet state lies too close to the $^4F_{9/2}$ emitting level of Dy(III) ion (Δ_E = 1400 cm^{-1}). This is confirmed by the weak emission observed in the spectrum of Dy(fod)$_3$ chelate in chloroform upon excitation within a π–π^* transition of fod. Therefore, the emission spectrum of [Dy$_2$(fod)$_6$(μ-bpm)] reveals that it is primarily sensitized by bpm due to its suitable energy difference with the $^4F_{9/2}$ emitting level of Dy(III) ion (Δ_E = 3000 cm^{-1}). However, the loss of energy due the interligand energy transfer as proposed for the terbium complex could also be responsible for the lower emission intensity of the dysprosium complex since the efficient sensitization of Dy(III) emission by bpm has been reported [53].

The emission spectrum of the praseodymium complex reveals that fod plays a major role in the sensitization process as compared to bpm since the emission intensity of $^1D_2$ transition of Pr(III) in the complex is slightly enhanced as compared to its intensity in Pr(fod)$_3$

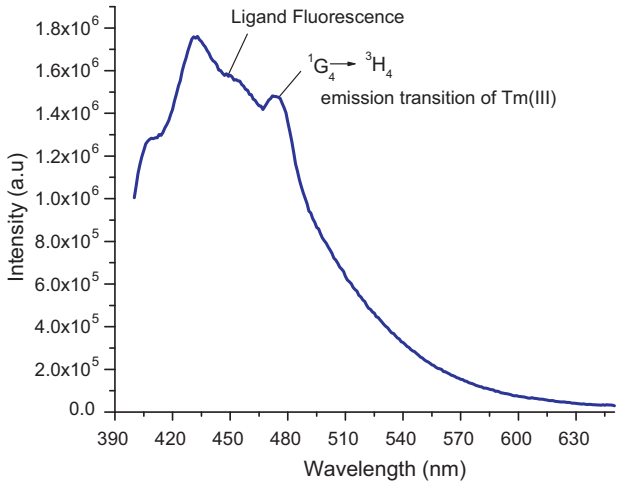

Fig. 11. Emission spectrum of $[Tm_2(fod)_6(\mu\text{-bpm})]$ in chloroform.

chelate. Furthermore, it has been reported that the emission properties of Pr(III) complexes can be controlled by the position of the triplet state of the ligand with respect to the $^3P_0$ and $^1D_2$ emitting levels of Pr(III) [45]. Since the triplet states of both fod and bpm lie well above the $^3P_0$ level (~20,600 cm^{-1}) (Δ_E = ~1900 cm^{-1} for fod and Δ_E = ~3500 cm^{-1} for bpm) and $^1D_2$ level (Δ_E = ~8160 cm^{-1} for fod and ~7260 cm^{-1} for bpm), it is remarkable that emission from both these levels is observed. However, it is surprising that despite a large energy difference between the triplet states of the ligands and the $^1D_2$ emitting level, the $^1D_2$ emission band is more prominent than the $^3P_0$ band. This is explained by the fact that there are two additional excited states above $^3P_0$ level of Pr(III) (Fig. 10) and these are $^1I_6$ (~21,350 cm^{-1}) and $^3P_1$ (~21,125 cm^{-1}) (Fig. 10). It is believed that the $^1I_6$, $^3P_1$, and $^3P_0$ excited states after receiving energy from the ligand centered triplet state rapidly transfer this energy to the $^1D_2$ emissive level of Pr(III) *via* non-radiative relaxation. The emission spectrum of the Pr(III) complex, also witnesses strong ligand fluorescence possibly from the coordinated bpm.

The emission spectrum of the chloroform solution of $[Tm_2(fod)_6(\mu\text{-bpm})]$ is dominated by the ligand fluorescence (Fig. 11). However, the shoulder at 474 nm in the broad fluorescence band matches with the $^1G_4 \rightarrow {}^3H_4$ blue emission transition of Tm(III), indicating a partial energy transfer from the coordinated ligands. A partial energy transfer from the triplet state of bpm to the $^1G_4$ emitting level of Tm (III) is also observed for $[Tm(NO_2)_3(bpm)_2]$ [53].

6. Conclusions

In this paper, dinuclear lanthanide complexes of the type $[Ln_2(fod)_6(\mu\text{-bpm})]$ (Ln = Nd–Lu) and polymeric complexes of the type $[Ln(fod)_3(bpm)]_n$ (Ln = La and Pr) have been isolated and thoroughly investigated in solution by ^1H NMR and steady-state emission studies. The ^1H NMR spectra of all the complexes and the respective chelates have been analysed in detail. The proton resonances of the coordinated bpm and fod ligands of the paramagnetic complexes are substantially shifted from their position in the diamagnetic complexes (La and Lu) while the magnitude and direction of the shift is dependent on the paramagnetic Ln(III) ions. The methine resonance of the paramagnetic complexes is shifted in opposite direction to the resonances of bpm and *tert*-butyl protons. The *tert*-butyl resonances are broader for the dinuclear complexes as compared to their precursor mononuclear chelates, reasonably due the twofold increase in the paramagnetic relaxation. The shift ratios of H-2 and H-3 proton resonances of the Sm, Eu and Er complexes are similar indicating that shifts are predominantly dipolar in nature and the three complexes are isostructural in solution. The steady-state emission spectra of the Pr, Sm, Eu, Tb, Dy and Tm complexes in chloroform are discussed by taking into consideration the triplet levels of the coordinated ligands and their energy match with the emitting levels of Ln(III) ions. The work emphasizes that the combination of fod and bpm is most effective for the sensitization of red and pink emissions of Eu(III) and Sm(III) ions, respectively. Despite bpm being an efficient sensitizer for the luminescence of Tb(III) and Dy(III) ions, a combination of bpm and fod is not much effective for the sensitization of these ions as compared to Eu(III) and Sm(III) ions. Among the many reasons including the energetic one, the depopulation of bpm centered excited states to the excited states of fod in terbium and dysprosium complexes could be one of the reasons.

Acknowledgements

We are thankful to Prof. T.R. Rao, Chemistry Department, Banaras Hindu University, Varanasi, India, for the measurement of the magnetic susceptibilities in his laboratory. MI thanks CSIR (Govt. of India) for Senior Research Fellowship.

Appendix A. Supplementary data

Supplementary data associated with this article can be found, in the online version, at doi:10.1016/j.jphotochem.2011.09.011.

References

[1] J.-C.G. Bünzli, C. Piguet, Chem. Soc. Rev. 34 (2005) 1048–1077.
[2] M.H.V. Werts, Sci. Prog. 88 (2005) 101–131.
[3] E. Brunet, J. Olga, J.C. Rodriguez-Ubis, Curr. Chem. Biol. 1 (2007) 11–39.
[4] J. Kido, Y. Okamoto, Chem. Rev. 102 (2002) 2357–2368.
[5] J.P. Leonard, C.M.G. dos Santos, S.E. Plush, T. McCabe, T. Gunnlaugsson, Chem. Commun. (2007) 129–131.
[6] S. Shinoda, H. Miyake, H. Tsukube, Molecular recognition and sensing via rare earth complexes, in: K.A. Gschneidner Jr., J.-C.G. Bünzli, V.K. Pecharsky (Eds.), Handbook on the Physics and Chemistry of Rare Earths, vol. 35, Elsevier, Amsterdam, 2005, pp. 273–335.
[7] K. Binnemans, C. Görller-Walrand, Chem. Rev. 102 (2002) 2303–2354.
[8] S. Faulkner, S.J.A. Pope, B.P. Burton-pye, Appl. Spectrosc. Rev. 40 (2005) 1–40.
[9] A.F. Cockerill, G.L.O. Davies, R.C. Harden, D.M. Reckham, Chem. Rev. 73 (1973) 553–588.
[10] K. Binnemans, Rare-earth beta-diketonates, in: K.A. Gschneidner Jr., J.-C.G. Bünzli, V.K. Pecharsky (Eds.), Handbook on the Physics and Chemistry of Rare Earths, vol. 35, Elsevier, Amsterdam, 2005, pp. 107–272.
[11] L.R. Melby, N.J. Rose, E. Abramson, J.C. Caris, J. Am. Chem. Soc. 86 (1964) 5117–5124.
[12] K. Iftikhar, M. Sayeed, N. Ahmad, Inorg. Chem. 21 (1982) 80–84.
[13] Z. Ahmed, K. Iftikhar, Inorg. Chim. Acta 363 (2010) 2606–2615.
[14] A.A. Ansari, M. Irfanullah, K. Iftikhar, Spectrochim. Acta A 67 (2007) 1178–1188.
[15] D.R. van Staveren, G.A. van Albada, J.G. Haasnoot, H. Kooijman, A.M.M. Lanfredi, P.J. Nieuwenhuizen, A.L. Spek, F. Ugozzoli, T. Weyhermüller, J. Reedijk, Inorg. Chim. Acta 315 (2001) 163–171.
[16] A. Bellusci, G. Barberio, A. Crispini, M. Ghedini, M. La Deda, D. Pucci, Inorg. Chem. 44 (2005) 1818–1825.
[17] M. Irfanullah, K. Iftikhar, Inorg. Chem. Commun. 13 (2010) 1234–1238.
[18] Y. Ma, G.-F. Xu, X. Yang, L.-C. Li, J. Tang, S.-P. Yan, P. Cheng, D.-Z. Liao, Chem. Commun. 46 (2010) 8264–8266.
[19] N.M. Shavaleev, S.J.A. Pope, Z.R. Bell, S. Faulkner, M.D. Ward, Dalton Trans. (2003) 808–814.
[20] M. Irfanullah, K. Iftikhar, Inorg. Chem. Commun. 12 (2009) 296–299.
[21] G. Zucchi, T. Jeon, D. Tondelier, D. Aldakov, P. Thuéry, M. Ephritikhine, B. Geffroy, J. Mater. Chem. 20 (2010) 2114–2120.
[22] G. Zucchi, O. Maury, P. Thuéry, M. Ephritikhine, Inorg. Chem. 47 (2008) 10398–10406.
[23] M.H. Baker, J.D. Dorweiler, A.N. Ley, R.D. Pike, S.M. Berry, Polyhedron 28 (2009) 188–194.
[24] N.M. Shavaleev, G. Accorsi, D. Virgili, Z.R. Bell, T. Lazarides, G. Calogero, N. Armaroli, M.D. Ward, Inorg. Chem. 44 (2005) 61–72.
[25] N.M. Shavaleev, Z.R. Bell, M.D. Ward, J. Chem. Soc. Dalton Trans. (2002) 3925–3927.
[26] M. Irfanullah, K. Iftikhar, J. Fluoresc. 21 (2011) 81–93.
[27] M. Irfanullah, K. Iftikhar, J. Fluoresc. 21 (2011) 673–686.
[28] M. Irfanullah, K. Iftikhar, J. Lumin. 130 (2010) 1983–1993.
[29] M. Irfanullah, K. Iftikhar, submitted for publication.

[30] C.S. Springer Jr., D.W. Meek, R.E. Sievers, Inorg. Chem. 6 (1967) 1105–1110.
[31] M. Julve, M. Verdaguer, G.D. Munno, J.A. Real, G. Bruno, Inorg. Chem. 32 (1993) 795–802.
[32] G.A. van Albada, W.J.J. Smeets, A.L. Spek, J. Reedijk, J. Chem. Crystallogr. 28 (1998) 427–432.
[33] A. Fratini, S. Swavey, Inorg. Chem. Commun. 10 (2007) 636–638.
[34] A. Fratini, G. Richards, E. Larder, S. Swavey, Inorg. Chem. 47 (2008) 1030–1036.
[35] S.V. Eliseeva, O.V. Kotova, F. Gumy, S.N. Semenov, V.G. Kessler, L.S. Lepnev, J.-C.G. Bünzli, N.P. Kuzmina, J. Phys. Chem. A 112 (2008) 3226–3614.
[36] K. Iftikhar, Polyhedron 15 (1996) 1113–1120.
[37] W.G.N. LaMar, W. De Horrocks Jr., R.H. Holm (Eds.), NMR of Paramagnetic Molecules, Academic Press, New York, 1973.
[38] N. Ishikawa, T. Iino, Y. Kaizu, J. Phys. Chem. A 107 (2003) 7879–7884.
[39] M. Gueron, J. Magn. Reson. 19 (1969) 58–66.
[40] A.J. Vega, D. Fiat, Mol. Phys. 31 (1976) 347–355.
[41] B.J. Bleaney, J. Magn. Reson. 8 (1972) 91–100.
[42] J.A. Fernandes, R.A. Sá Ferreira, M. Pillinger, L.D. Carlos, J. Jepsen, A. Hazel, P.R. Claro, I.S. Gonçalves, J. Lumin. 113 (2005) 50–63.
[43] Y. Hasegawa, S-i. Tsuruoka, T. Yoshida, H. Kawai, T. Kawai, J. Phys. Chem. A 112 (2008) 803–807.
[44] F.S. Richardson, Chem. Rev. 82 (1982) 541–552.
[45] F. Gu, S.F. Wang, M.K. Lu, G.J. Zhou, D. Xu, D.R. Yuan, Langmuir 20 (2004) 3528–3531.
[46] A.I. Voloshin, N.M. Shavaleev, V.P. Kazakov, J. Lumin. 93 (2001) 199–204.
[47] M.D. Regulacio, M.H. Pablico, J.A. Vasquez, P.N. Myers, S. Gentry, M. Prushan, S.-W. Tam-Chang, S.L. Stoll, Inorg. Chem. 47 (2008) 1512–1523.
[48] A. Ishii, S. Kishi, H. Ohtsu, T. Iimori, T. Nakabayashi, N. Ohta, N. Tamai, M. Melnik, M. Hasegawa, Y. Shigesato, ChemPhysChem 8 (2007) 1345–1351.
[49] W.T. Carnall, P.R. Fields, K. Rajnak, J. Chem. Phys. 49 (1968) 4424–4442.
[50] W.T. Carnall, P.R. Fields, K. Rajnak, J. Chem. Phys. 49 (1968) 4447–4449.
[51] W.T. Carnall, P.R. Fields, K. Rajnak, J. Chem. Phys. 49 (1968) 4450–4455.
[52] M. Latva, H. Takalo, V.M. Mukkala, C. Matachescu, J.C. Rodríguez-Ubis, J. Kankare, J. Lumin. 75 (1997) 149–169.
[53] G. Zucchi, O. Maury, P. Thuéry, F. Gumy, J.-C.G. Bünzli, M. Ephritikhine, Chem. Eur. J. 15 (2009) 9686.
[54] F.J.P. Schuurmans, A. Lagendijk, J. Chem. Phys. 113 (2000) 3310–3314.
[55] Z.-F. Li, L. Zhou, J.-B. Yu, H.-J. Zhang, R.-P. Deng, Z.-P. Peng, Z.-Y. Guo, J. Phys. Chem. C 111 (2007) 2295–2300.